CHAPTER VII
EFFECT OF CASTING SOLVENT ON CHARACTERISTICS OF HEXANOYL CHITOSAN/POLYLACTIDE BLEND FILMS

7.1 ABSTRACT

Blend films of hexanoyl chitosan (H-chitosan) and polylactide (PLA) were cast from corresponding blend solutions in chloroform, dichloromethane, or tetrahydrofuran. Thermal degradation behavior of the as-prepared blend films was intermediate to those of the pure components and no significant effect from the type of the casting solvent using was observed. All of the blend films exhibited one composition-dependent glass transition temperature, but the results only suggested partial miscibility of the components in the amorphous at "low" contents of H-chitosan. As revealed by solvent etching technique, the as-prepared blend films cast from blend solutions in chloroform and dichloromethane show extensive phase separation of the two components, with the minor phase being formed into discrete domains throughout the matrix. Both thermal and X-ray analyses showed that the apparent degree of crystallinity of the PLA component in the blends decreased monotonically with increasing H-chitosan content and the choice of the cast solvent did not have an effect on the structure of PLA crystals.

(**Key-words**: hexanoyl chitosan; polylactide; polymer blend; casting solvent effect)

7.2 INTRODUCTION

Polymer blending is an attractive route for producing new polymeric materials with tailored properties without having to synthesize totally new materials. Other advantages for polymer blending are versatility, simplicity, and inexpensiveness. Physical and mechanical properties of the blends are very much dependent on state of mix and miscibility between the constituent components as well as the phase morphology of the resulting blends. For solution-cast blends however, another important factor determining the final properties of the resulting blends is the choice of the casting solvent used to prepare the blend solutions for casting.

Even though a large number of studies on solution-cast polymer blends are available in the open literature, only limited number are dedicated to study the effect of casting solvent on properties of the resulting blends. Bank *et al.* [1] showed that films of polystyrene (PS)/poly(vinyl methyl ether) (PVME) blends appeared to be compatible when either toluene or benzene was use as the casting solvent, and they appeared to be incompatible when either trichloroethylene or chloroform was used. Asaletha *et al.* [2] reported that the nature of the casting solvent had a profound effect on the compatibility behavior of natural rubber (NR)/polystyrene (PS) blends compatibilized by NR-g-PS. Radhakrishnan and Venkatachalapathy [3] showed that the choice of the casting solvent used (e.g. dichloromethane, tetrahydrofuran, and toluene) to prepare the blend films of poly(ethylene oxide) (PEO) and poly(methyl methacrylate) (PMMA) not only affected the compatibility of the resulting films, but also the crystallization of PEO.

Also working with PEO/PMMA blends, Liau and Chang [4] showed that PEO/PMMA blends were miscible when either benzene or chloroform was chosen as the casting solvent and that crystallization of PEO was found to be more suppressed when chloroform was selected. In blends of poly(vinyl acetate) (PVA) and PEO, Wu *et al.* [5] reported that the resulting blends were miscible when benzene was used as the casting solvent and that crystallization of PEO was more easily suppressed when benzene was instead used, as evidenced by the fact that the interaction parameter of benzene-cast films showed a greater negative value than that of chloroform-cast

ones. Tang and Liau [6] studied the effect of casting solvent (e.g. acetone, tetrahydrofuran, isopropyl acetate, *n*-butanol, or cyclohexanone) on morphology and properties of poly(4-hydroxystyrene) and PEO blends and reported that, regardless of the solvent type, the blends were miscible as evidenced by a single glass transition temperature observed and that crystallization of PEO was more suppressed when either tetrahydrofuran or cyclohexanone was used as the casting solvent.

In the present contribution, blend films of hexanoyl chitosan (H-chitosan) and PLA were prepared by the solution-casting technique. The effect of casting solvent (chloroform, dichloromethane, or tetrahydrofuran) on physical, thermal, and phase behavior of the resulting blend products was investigated and reported.

7.3 EXPERIMENTAL

Materials

Chitosan having the degree of deacetylation of about 91% was prepared from shrimp shells by acid and alkali treatments. Chitosan was pulverized into powder, the size of which ranged from 71 to 75 μm, prior to further use. Hexanoyl chitosan (H-chitosan) was synthesized by reacting chitosan powder with hexanoyl chloride (Fluka, Switzerland) in a mixture of anhydrous pyridine (Sigma-Aldrich, USA) and chloroform (Sigma-Aldrich, USA), according to Figure 7.1 [7]. PLA was courteously supplied by Daiseru Chemicals (Japan). The viscosity-average molecular weight $\overline{M}_v$ of PLA was determined, based on viscosity measurements at 25°C in chloroform following the Mark-Houwink equation of the form [8]: $[\eta] = 7.4 \times 10^{-5} \cdot \overline{M}_v^{0.87}$, to be ca. 70,000 g·mol^{-1}. Chloroform, dichloromethane, and tetrahydrofuran, used as the casting solvents, were purchased from Labscan (Asia) (Thailand).

Preparation of Blend Films

To prepare H-chitosan/PLA blend films, solutions of H-chitosan and PLA were separately prepared at the concentration of 1% w/w, using chloroform, dichloromethane, or tetrahydrofuran as the solvent. Slight stirring was used to

expedite the dissolution and to homogenize the solutions. Blends films of different compositions (i.e. the weight ratios between H-chitosan and PLA of 100/0, 80/20, 60/40, 50/50, 40/60, 20/80, and 0/100, respectively) were prepared by casting a mixture of the solutions of a specified composition on a Teflon dish. Each cast film was let dry at room temperature for one day and later at room temperature *in vacuo* for another two days.

Characterization Techniques

Thermal properties of pure and the as-prepared blend products were analyzed by thermogravimetric analysis (TGA) and differential scanning calorimetry (DSC). TGA patterns were measured on a Perkin-Elmer Diamond TG/DTA analyzer at a heating rate of 10°C·min^{-1} under nitrogen atmosphere over a scanning range of 30 to 750°C. Samples of about 10 to 20 mg were used for TGA analysis. Observation of the glass transition temperature (T_g) and melting characteristic of the as-cast pure and blend products were analyzed by DSC and the crystallization characteristic was also by wide-angle X-ray diffraction (WAXD). DSC thermograms were recorded on a Mettler DSC 822e/400 analyzer at a heating rate of 10°C·min^{-1} under nitrogen atmosphere. It should be noted that the 20 μl pans (1 to 2 mg of samples) were used for the T_g measurements and the standard 40 μl pans (3 to 4 mg of samples) were used for observing the crystallization characteristic of the samples. WAXD patterns were recorded on a Rigaku Rint2000 X-ray diffractometer. The X-ray source was Cu Kα. The scanning range and the scanning speed were 5 to 40° and 5 deg·sec^{-1}, respectively. Phase morphology of the as-prepared blend films was investigated by a JEOL 520-2AE scanning electron microscope (SEM). Prior to observation under SEM, the blend films were either etched with cyclohexane or concentrated acetic acid solution for two minutes at room temperature in order to remove H-chitosan or PLA, respectively.

7.4 RESULTS AND DISCUSSION

Physical Appearance

Table 7.1 summarizes physical appearance of the as-prepared films of pure H-chitosan, pure PLA, and H-chitosan/PLA blends, using chloroform, dichloromethane, or tetrahydrofuran as the casting solvent. Generally, blend films cast from blend solutions in chloroform and dichloromethane appeared similar in their physical appearance. On the contrary, blend solutions in tetrahydrofuran could not be cast into films when PLA content was greater than 20 wt.%. Pure H-chitosan films appeared to be elastic (when dichloromethane was used) or even sticky (when chloroform was used), while pure PLA films appeared to be quite brittle. Interestingly, blend films exhibited characteristics intermediate to those of the pure components, becoming more ductile with increasing H-chitosan content, or vice versa.

Such physical appearance of the as-cast products could be explained based on the physicochemical properties of the solvents used. Among the various properties, boiling point (T_b) and Hildebrand solubility parameter (δ) of the solvent should be the most important. T_b values of chloroform, dichloromethane, and tetrahydrofuran are about 61, 40, and 66°C, respectively, while δ values are about 9.2, 9.6, and 9.1 $cal^{0.5} \cdot cm^{-1.5}$, respectively [9]. In comparison, the δ values for H-chitosan (assuming full substitution of the hexanoyl groups) and PLA were calculated based on the group contribution method of van Krevelen [10] to be about 9.3 and 9.4 $cal^{0.5} \cdot cm^{-1.5}$, respectively. Based on these δ values, it is quite obvious that mixed solutions of H-chitosan and PLA in either chloroform or dichloromethane should appear to be miscible, while those in tetrahydrofuran should be less miscible.

Thermal Characteristics

Thermal Degradation

Thermal stability of pure H-chitosan, pure PLA, and corresponding blend products was evaluated by TGA technique. Table 7.2 summarizes the observed degradation peak value(s) (denoted T_d) for all of the films investigated. According to

the derivative TGA curves, pure PLA products cast from solutions in chloroform, dichloromethane, or tetrahydrofuran showed one degradation peak at about 327, 354, and 320°C, respectively, while pure H-chitosan films exhibited two degradation peaks at about 257 and 327, 261 and 329, and 262 and 325°C, respectively. Obviously, thermal stability of pure H-chitosan films was not affected by the choice of the casting solvent used. Figure 7.2 shows TGA patterns for 50/50 w/w H-chitosan/PLA blend products cast from blend solutions in chloroform, dichloromethane, or tetrahydrofuran, respectively. Apparently, two-step weight loss were observed for these blend products. The observation was general for all of the blends investigated, in which two degradation peaks were observed (see Table 7.2) and thermal degradation behavior of the blend products at a given blend composition did not seem to be affected by the choice of the casting solvent used.

Glass Transition Temperature

One important parameter used to investigate whether two polymers are miscible in the amorphous phase is the glass transition temperature (T_g). It is also well known that, for semi-crystalline polymers, T_g is quite difficult to measure. Indeed, the rigid amorphous phase, located between the lamellae and the bulk amorphous phase, does not transform into a mobile, amorphous liquid phase at T_g and is not quite observable by a common DSC in the usual conditions used for its measurement. Since this rigid amorphous interfacial region often accounts to a great extent to the discrepancies in the measurement of the crystalline and the bulk amorphous contents, polymers are usually quenched from the melt to a temperature situated well below T_g to decrease its importance.

In DSC, the miscibility of two polymers in the bulk amorphous phase can be evaluated by the presence of a single, composition-dependent T_g value between those of the constituent polymers. In order to measure the T_g for the as-prepared blends, each blend sample was heated from room temperature to 200°C at a heating rate of 10°C·min^{-1}. After thermal equilibration, the sample was taken out from the DSC furnace, while in the sample holder, and was quenched in liquid nitrogen to maximize the bulk amorphous content in the sample. After 20 min of submersion in

liquid nitrogen, the sample was put back into the DSC furnace, the temperature of which was equilibrated at room temperature, and a second heating scan was subsequently carried out as soon as the temperature of the sample equilibrated to that of the DSC furnace. The T_g was then measured on this second heating scan. Figure 7.3 illustrates the observed T_g values for pure PLA and corresponding blend products cast from solutions in different solvents. It should be note that the T_g for pure H-chitosan could not be observed within the temperature range investigated.

No obvious T_g was observed in the DSC thermogram obtained for pure H-chitosan films, while the T_g values of about 61, 57 and 59°C was observed for pure PLA products cast from solutions in chloroform, dichloromethane, and tetrahydrofuran, respectively. The observed T_g values for PLA were in agreement with the value of 56°C observed by thermomechanical analysis [10]. In all of the blend products investigated, a single, compositional dependent T_g was clearly observed. Apparently, the observed T_g values of the blends did not seem to exhibit a strong relationship with the blend composition. Even though, at a given blend composition, all of the blend products showed only one T_g, it was not possible to conclude with a certain level of confidence that H-chitosan and PLA molecules were miscible in the amorphous phase, since, within the temperature range investigated, the T_g for pure H-chitosan could not be observed. However, at "low" H-chitosan contents (i.e. $\leq$ 40 wt.%), the observed slight decrease in the T_g values of the blend products from that of pure PLA samples (see Figure 7.3) could be a result of the partial miscibility of H-chitosan and PLA molecules in the amorphous phase and the observed slight increase in the T_g values of the blend products with further increase in the H-chitosan content could be due to the restricted mobility of PLA molecules in the presence of H-chitosan molecules as the major phase.

Melting Behavior and Apparent Degree of Crystallinity

Prior to observing the melting behavior and the apparent degree of crystallinity, each sample was pre-conditioned in the same manner in order to set the thermal history of the sample by heating each sample from room temperature to 200°C at a heating rate of 10°C·min^{-1} and immediately cooling it down at a cooling

rate of 10°C·min^{-1} to room temperature. The thermogram for the second heating scan was recorded for further analysis.

Figure 7.4 shows heating thermograms for pure H-chitosan, pure PLA, and H-chitosan/PLA blend products which were cast from solutions in different solvents. Evidently, no thermal transition of any kind was discernable in the heating thermogram for pure H-chitosan. For both pure PLA and corresponding blend products of various compositions, either one or two melting endotherm(s) was observed. Based on related studies on the multiple-melting behavior of some other semi-crystalline polymers [11,12], the occurrence of the low-temperature melting endotherm (T_{ml}) was usually attributed to the melting of the primary crystals formed during the first cooling, while that of the high-temperature melting endotherm (T_{mh}) was to the melting of the re-crystallized crystals formed during a heating scan.

These values for all of the pure PLA and H-chitosan/PLA blend samples investigated are summarized in Table 7.3. Apparently, the T_{ml} values for all of the blend samples were slightly lower than those of the pure PLA ones, but no significant dependency of these values on H-chitosan content was observed. Since it is now a general knowledge that depression of both the apparent and the equilibrium melting temperatures is expected, if the blending polymer pairs are somewhat miscible [5,6,13]. As a result, the observed slight decrease in the T_{ml} values with initial addition of H-chitosan and the observed constancy in the T_{ml} values with further increase in the H-chitosan content suggested that H-chitosan and PLA were partially miscible at "low" H-chitosan contents (i.e. ≈20 wt.%) and became more immiscible when H-chitosan content increased.

Another important information which can be deduced from the thermograms shown in Figure 7.4 is the apparent degree of crystallinity that was present in each of the as-cast films. Qualitatively, the area under the melting endotherm related directly to the amount of the crystals present within the samples that were cast from solutions of different solvents. Since the high-temperature melting endotherm related to the melting of the re-crystallized crystals, only the low-temperature melting one should only be accounted for the amount of the crystals present within each sample. According to Figure 7.4, the fractional area of the low-temperature melting

endotherm for samples cast from solutions of each respective solvent decreased monotonically with increasing H-chitosan content, most likely a result of the dilution effect at higher H-chitosan contents.

In order to quantitatively analyzed the results obtained, the enthalpy of fusion values specific to the low-temperature melting endotherm (ΔH_f) for all of the samples investigated are summarized in Table 7.4. Based on the results obtained, the apparent degree of crystallinity χ_c of each sample can be approximated according to the following equation:

$$\chi_c(\%) = \frac{\Delta H_f}{\Delta H_f^0 \cdot w_{PLA}} \times 100 \quad (1)$$

where ΔH_f^0 is the equilibrium enthalpy of fusion for PLA (i.e. 93 $J \cdot g^{-1}$ [14]) and w_{PLA} is the weight fraction of PLA in the as-cast sample. The calculated value of χ_c for each film prepared is also summarized in Table 7.4. Apparently, the χ_c value for samples cast from solutions of each respective solvent decreased with increasing H-chitosan content, with, for a given H-chitosan content, the samples cast from the blend solutions in dichloromethane exhibiting the highest χ_c value among the samples investigated.

Morphological Characteristics

In order to clearly observe the phase morphology of H-chitosan and PLA in the as-cast blend films, each blend film (only for that cast from blend solutions in chloroform or dichloromethane) was either etched in cyclohexane to remove H-chitosan or a concentrated acetic acid solution to remove PLA when the corresponding component was the minor phase in the blend film.

Figure 7.5 shows SEM images illustrating the surface morphology of the as-etched blend films having H-chitosan content being 20 and 40 wt.%. Figure 7.5a-b shows SEM images of the blend films cast from blend solutions in chloroform, while Figure 7.5c-d shows SEM images of the blend films cast from blend solutions in dichloromethane. The voids observed were H-chitosan particles which were dissolved away after the blend films were immersed in cyclohexane for two minutes. From these images, H-chitosan and PLA were found to phase-separate during the

evaporation of the solvent. When H-chitosan was the minor phase, the H-chitosan particles were found to distribute quite regularly throughout the PLA matrix and the size of the particles decreased, while the number of the particles increased, with increasing amount of H-chitosan from 20 to 40 wt.%. Interestingly, the blend films cast from blend solutions in dichloromethane showed much higher number of H-chitosan particles than those in chloroform, suggesting that the blend films cast from blend solutions in dichloromethane should be less miscible that those in chloroform.

Figure 7.6 shows SEM images illustrating the surface morphology of the as-etched blend films having PLA content of 20 and 40 wt.%. Figure 7.6a-b shows SEM images of the blend films cast from blend solutions in chloroform, while Figure 7.6c-d shows SEM images of the blend films cast from blend solutions in dichloromethane. The voids present in these images were PLA particles which were dissolved away after the blend films were immersed in a concentrated acetic acid solution for two minutes. For the blend films cast from blends solution in chloroform, the PLA minor phase was found to distribute very regularly throughout the H-chitosan matrix and the size of the particles increased, while the number of the particles decreased, with increasing PLA content 20 to 40 wt.%. On the contrary, the PLA particles in the blend films cast from blend solutions in dichloromethane distributed quite evenly throughout the H-chitosan matrix and the size of the particles decreased, while the number of the particles increased, with increasing amount of PLA from 20 to 40 wt.%.

The difference in the surface morphology of the as-etched blend films cast from blend solutions in different solvents could be attributed to the difference in the boiling points and the Hildebrand solubility parameters (in comparison with those of H-chitosan and PLA). Since the boiling point of dichloromethane (i.e. 40°C) was much lower than that of chloroform (i.e. 61°C), while the solubility parameters were not much different when comparing with those of H-chitosan and PLA, the minor phase being present in the blend films from dichloromethane should be more irregular when comparing with that in the blend films from chloroform.

Crystalline Structure

WAXD patterns for pure H-chitosan, pure PLA, and all of the blend films cast from solutions in either chloroform or dichloromethane investigated are illustrated in Figure 7.7. Obviously, the WAXD pattern for pure H-chitosan films from both solvents exhibited a sharp diffraction peak at the scattering angle 2θ of around 6.0° along with a broad diffraction peak centering at the 2θ of around 18.7°. The sharp diffraction peak at about 6.0° was reported to be a result of the interdegitation of the hexanoyl side-chains with the extended main chains forming a layer structure, while the broad diffraction peak at about 18.7° was a result of the loss of crystallinity due to the loss of hydrogen bonding [7]. For pure PLA film cast from PLA solution in chloroform, the obtained WAXD pattern showed only one broad diffraction peak centering at the 2θ of around 16.9°, while that from PLA solution in dichloromethane showed relatively sharp diffraction peaks at the 2θ's of about 17 and 19°. When crystallizing in a pseudo-orthorhombic unit cell (with axes a = 1.07 nm, b = 0.595 nm, and c = 2.78 nm), PLA should show main diffraction peaks at the 2θ's of 15, 17, and 19° [15]. For H-chitosan/PLA blend films, the obtained diffraction patterns appeared to contain the diffraction peaks characteristic to both pure H-chitosan and pure PLA. No significant shift in the diffraction peaks was observed, suggesting that the presence of one component did not affect the ordered structure which would be observed for the other component. Apparently, the blend films cast from solutions in dichloromethane exhibited greater apparent degree of crystallinity (for the blend films having PLA contents of greater than 60 wt.%) than those in chloroform. The results were in excellent agreement with the observation by DSC.

7.5 CONCLUSIONS

Blend products of hexanoyl chitosan (H-chitosan) and polylactide (PLA) were prepared by the solution-casting technique from different solvents, such as chloroform, dichloromethane or tetrahydrofuran. Only the blend solutions in chloroform and dichloromethane could be cast into films at all blend compositions.

The thermal degradation behavior of the as-prepared blend films was found to be intermediate to those of the pure components and no significant effect on the type of the casting solvent was observed. All of the blend products exhibited one composition-dependent glass transition temperature (T_g). The observed slight decrease in the T_g values of the blend products of "low" H-chitosan contents (i.e. $\leq$ 40 wt.%) from that of pure PLA samples suggested partial miscibility of H-chitosan and PLA molecules in the amorphous phase at these compositions.

With the temperature range investigated, pure H-chitosan films showed no thermal transition of any kind, while both PLA and corresponding blend products of various compositions exhibited either one or two melting endotherm(s). It was postulated that the occurrence of the low-temperature melting endotherm was a result of the melting of the primary crystals of PLA formed during cooling. The observed decrease in the peak temperature of this endotherm for blend products of "low" H-chitosan contents (i.e. $\approx$20 wt.%) suggested partial miscibility of H-chitosan and PLA molecules in the amorphous phase at these compositions, while the observed decrease in the area under this endotherm with increasing H-chitosan content suggested decreased apparent degree of crystallinity of PLA component in the blends. Such observation on the apparent degree of crystallinity also confirmed by the results from the X-ray analysis.

7.6 ACKNOWLEDGMENTS

The authors wish to thank partial support from the Petroleum and Petrochemical Technology Consortium (through a governmental load from the Asian Development Bank), Chulalongkorn University (through a research grant from the Ratchadaphisek Somphot Endowment Fund) and the Petroleum and Petrochemical College, Chulalongkorn University.

7.7 REFERENCES

[1] Bank, M.; Leffingwell, J.; Thies, C. *Macromolecules* 1971, 4, 43.

[2] Asaletha, R.; Kumaran, M. G.; Thomas, S. *Polymer – Plastics Technology and Engineering* 1995, 34, 633.

[3] Radhakrishnan, S.; Venkatachalapathy, P. D. *Polymer* 1996, 37, 3749.

[4] Liau, W. B.; Chang, C. F. *Journal of Applied Polymer Science 2000*, 76, 1627.

[5] Wu, W. B.; Chiu, W. Y.; Liau, W. B. *Journal of Applied Polymer Science* 1997, 64, 411.

[6] Tang, M.; Liau, W. R. *European Polymer Journal* 2000, 36, 2597.

[7] Zong, Z.; Kimura, Y.; Takahashi, M.; Yamane, H. *Polymer* 2000, 41, 899.

[8] Rafler, G.; Dahlmann, J.; Wiener, K. *Acta Polymerica* 1990, 41, 328.

[9] van Krevelen, D.W. in Properties of polymers: their correlation with chemical structure; their numerical estimation and prediction from additive group contributions; Eisevier Science: Amsterdam, 1997; 3rd ed; pp 213 - 219.

[10] Liu, C.; Mather, P. T. *Journal of Applied Medical Polymers* 2002, 6, 47.

[11] Supaphol, P. *Journal of Applied Polymer Science* 2001, 82, 1083.

[12] Srimoaon, P.; Dangseeyun, N.; Supaphol, P. *European Polymer Journal* 2004, 40, 599.

[13] Nishi, T.; Wang, T. T. *Macromolecules* 1975, 8, 909.

[14] Fischer, E. W.; Sterzel, H. J.; Wegner, G. *Kolloid-Zeitschrift and Zeitschrift fur Polymere* 1973, 251, 980.

[15] Kister, G.; Cassanas, G.; Vert, M. *Polymer* 1998, 39, 267.

7.8 CAPTION OF FIGURES

Figure 7.1 A synthesis route for perfect H-chitosan.

Figure 7.2 TGA curves for 50/50 w/w H-chitosan/PLA blend products cast from blend solutions in different solvents: (a) chloroform, (b) dichloromethane, and (c) tetrahydrofuran. The heating rate used was $10°C \cdot min^{-1}$.

Figure 7.3 Observed glass transition temperature for pure PLA and H-chitosan/PLA blend products cast from blend solutions in different solvents: (○) chloroform, (▽) dichloromethane, and (□) tetrahydrofuran; plotted as a function of H-chitosan content.

Figure 7.4 Second heating thermogram for pure H-chitosan, pure PLA, and H-chitosan/PLA blend products cast from blend solutions in different solvents: (a) chloroform, (b) dichloromethane, and (c) tetrahydrofuran.

Figure 7.5 Scanning electron micrographs for as-etched H-chitosan/PLA blend films with the weight ratios of (a) 20/80, (b) 40/60, (c) 20/80, and (d) 40/60, respectively. Figures (a-b) are for films cast from blend solutions in chloroform, while Figures (c-d) in dichloromethane.

Figure 7.6 Scanning electron micrographs for as-etched H-chitosan/PLA blend films with the weight ratios of (a) 80/20, (b) 60/40, (c) 80/20, and (d) 60/40, respectively. Figures (a-b) are for films cast from blend solutions in chloroform, while Figures (c-d) in dichloromethane.

Figure 7.7 Wide-angle X-ray diffraction pattern for pure H-chitosan, pure PLA, and H-chitosan/PLA blend films cast from blend solutions in different solvents: (a) chloroform, and (b) dichloromethane.

Table 7.1 Appearance of pure H-chitosan and H-chitosan/PLA blend products casting from blend solutions in different solvents

H-chitosan/PLA blend composition	Solvent		
	Chloroform	Dichloromethane	Tetrahydrofuran
100/0	Sticky-opaque film	Elastic-opaque film	Elastic-opaque film
80/20	Sticky-opaque film	Elastic-opaque film	Elastic-opaque film
60/40	Elastic-opaque film	Elastic-opaque film	Non-film
50/50	Elastic-opaque film	Elastic-opaque film	Non-film
40/60	Elastic-opaque film	Opaque film	Non-film
20/80	Opaque film	Brittle-opaque film	Non-film
0/100	Brittle-clear film	Brittle-clear film	Non-film

Table 7.2 Thermal decomposition temperature(s) of pure H-chitosan, pure PLA, and H-chitosan/PLA blend products cast from blend solutions in different solvents

H-chitosan/PLA blend composition	Chloroform		Dichloromethane		THF	
	1^{st} T_d (°C)	2^{nd} T_d (°C)	1^{st} T_d (°C)	2^{nd} T_d (°C)	1^{st} T_d (°C)	2^{nd} T_d (°C)
0/100	-	327±2	-	354±0	-	320±1
20/80	-	336±0	263±0	338±0	-	319±3
40/60	264±0	316±1	260±1	318±2	263±0	322±0
50/50	254±1	312±2	258±1	317±2	260±0	321±3
60/40	255±3	313±1	260±0	313±0	255±3	319±1
80/20	257±2	309±1	261±2	311±1	258±0	318±1
100/0	257±0	327±2	261±2	329±1	262±2	325±3

Table 7.3 Low-temperature melting peak and high-temperature melting peak of PLA component in pure H-chitosan, pure PLA, and H-chitosan/PLA blend products casting from blend solutions in different solvents

H-chitosan/PLA blend composition	Chloroform		Dichloromethane		Tetrahydrofuran	
	T_{ml} (°C)	T_{mh} (°C)	T_{ml} (°C)	T_{mh} (°C)	T_{ml} (°C)	T_{mh} (°C)
0/100	162	170	163	168	162	169
20/80	158	168	160	170	158	167
40/60	159	168	160	169	156	165
50/50	159	168	160	169	156	166
60/40	160	168	160	168	158	167
80/20	-	168	-	169	-	166
100/0	-	-	-	-	-	-

Table 7.4 Enthalpy of fusion specific to the low-temperature melting endotherm and corresponding apparent degree of crystallinity of PLA component in pure H-chitosan, pure PLA, and H-chitosan/PLA blend products casting from blend solutions in different solvents

H-chitosan/PLA blend composition	Chloroform		Dichloromethane		Tetrahydrofuran	
	ΔH_f (J/g)	χ_c (%)	ΔH_f (J/g)	χ_c (%)	ΔH_f (J/g)	χ_c (%)
0/100	21.7±0.2	23.3±0.2	32.6±0.9	35.0±1.0	19.5±0.7	21.0±0.8
20/80	9.6±0.8	12.9±4.3	17.6±0.3	23.7±1.6	14.4±0.9	19.3±4.8
40/60	6.9±0.8	12.4±2.2	10.5±0.5	18.9±1.3	7.4±0.8	13.2±2.2
50/50	3.7±0.4	7.9±0.9	8.6±0.8	18.4±1.7	5.4±0.5	11.6±1.1
60/40	3.3±0.9	8.9±1.6	6.8±0.6	18.2±1.1	3.8±0.4	10.1±0.7
80/20	1.5±0.7	8.2±0.9	3.1±0.0	16.6±0.0	1.5±0.9	8.2±1.2
100/0	-	-	-	-	-	-

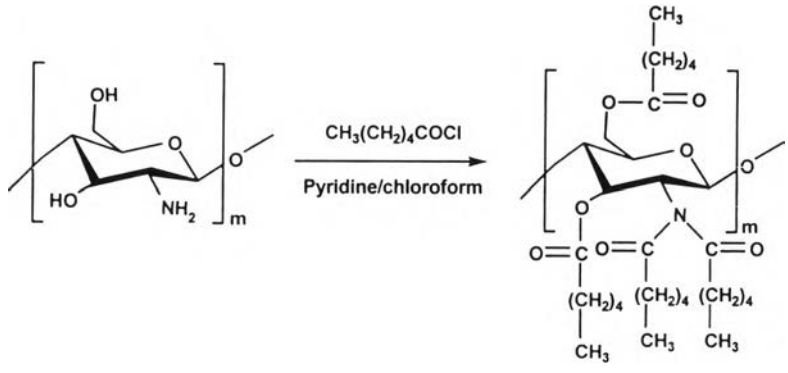
OH
HO
NH2
m
CH3(CH2)4COCl
Pyridine/chloroform
CH3
(CH2)4
O
C
O
N
m
(CH2)4
CH3

Figure 7.1

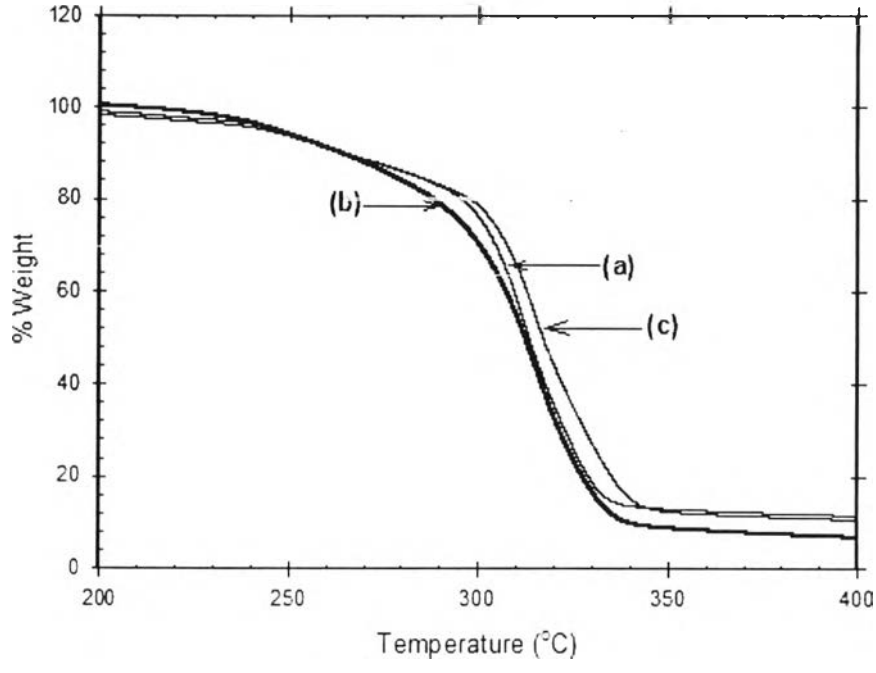
120
100
80
60
40
20
0
% Weight
200
250
300
350
400
Temperature (°C)
(b)
(a)
(c)

Figure 7.2

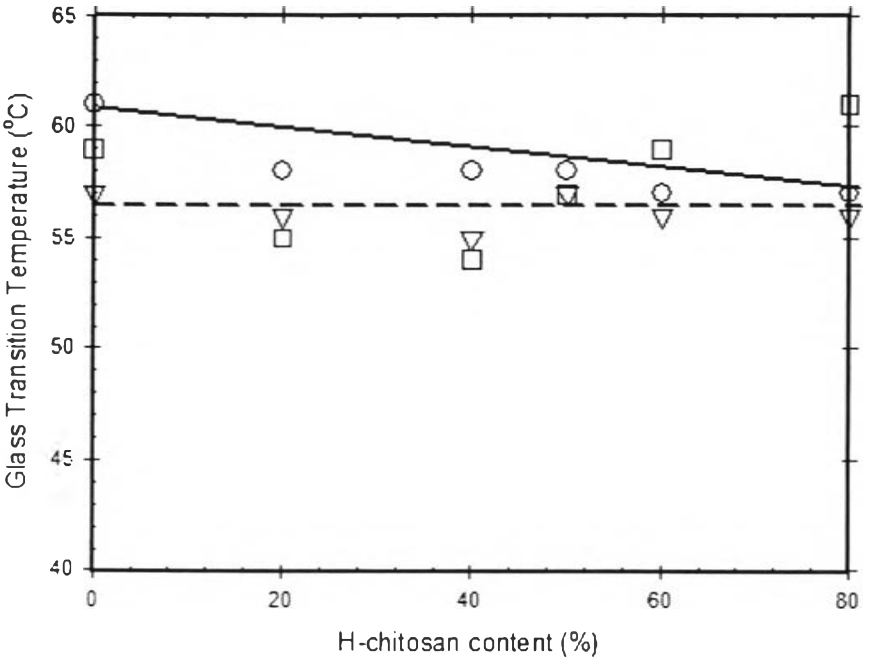
65
60
55
50
45
40
Glass Transition Temperature (°C)
0
20
40
60
80
H-chitosan content (%)

Figure 7.3

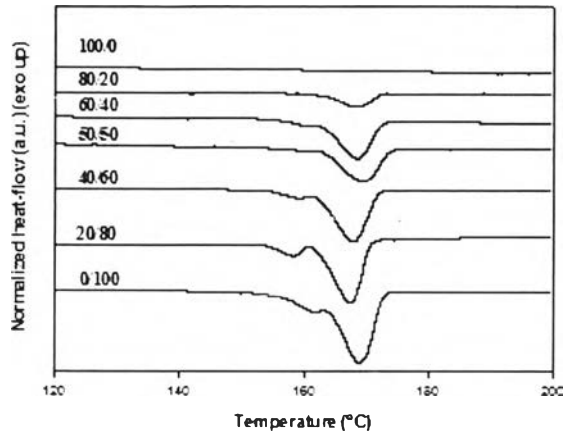

(a)

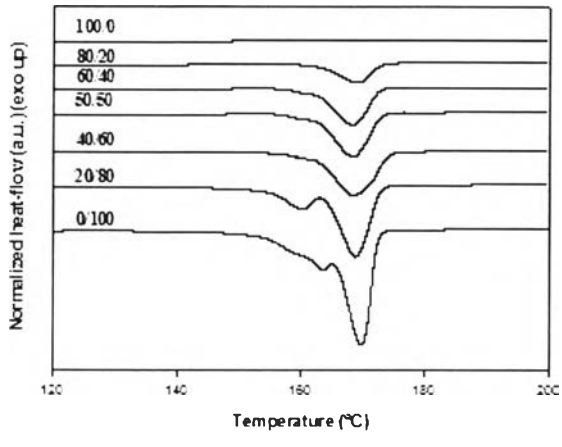

(b)

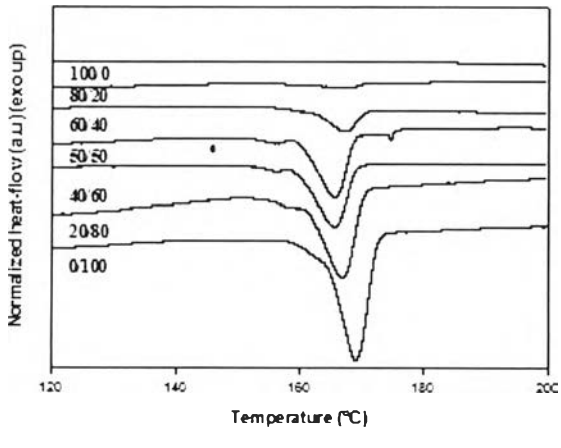

(c)

Figure 7.4

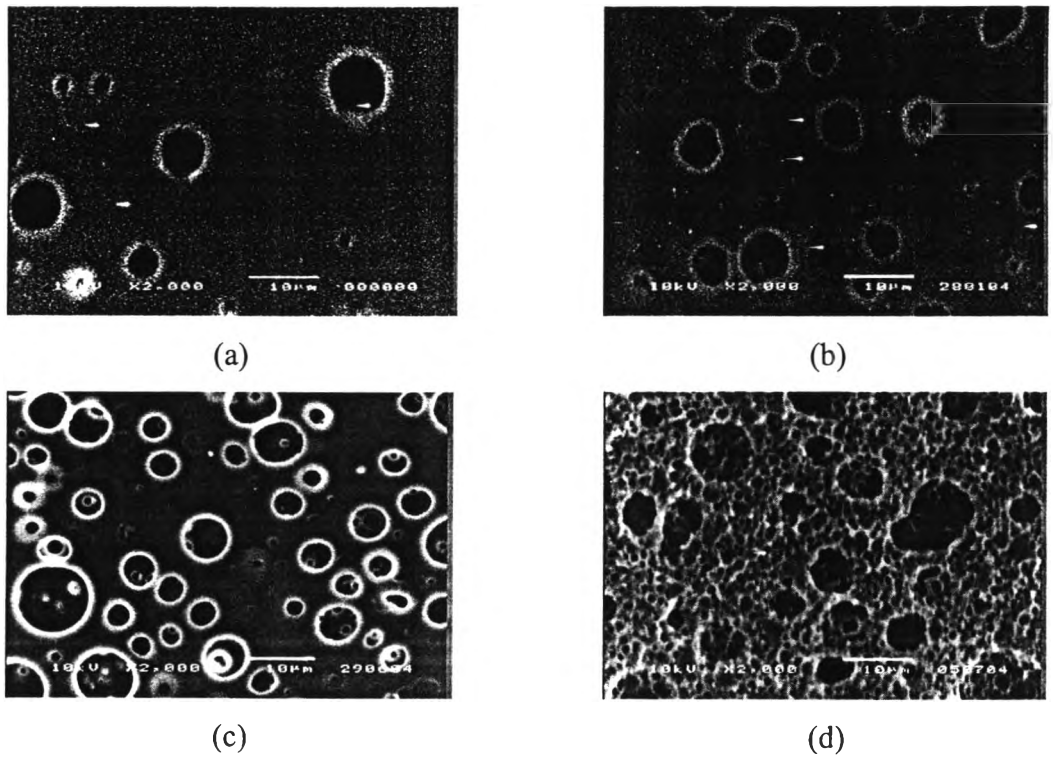

(a) (b)

(c) (d)

Figure 7.5

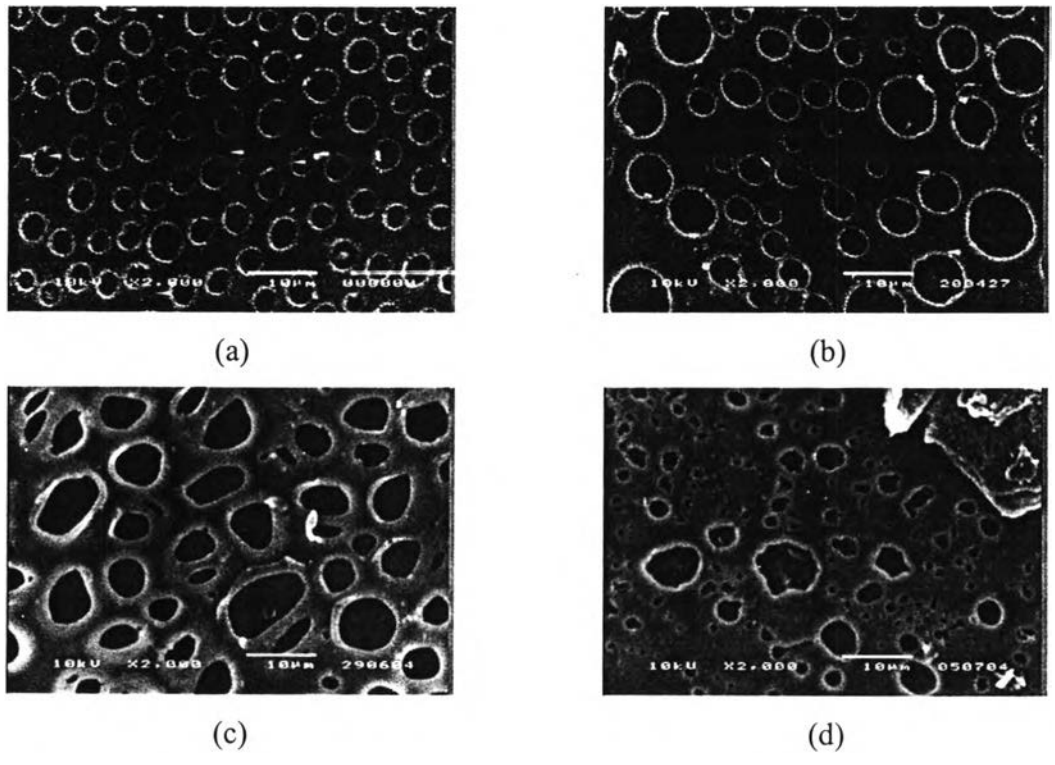

Figure 7.6

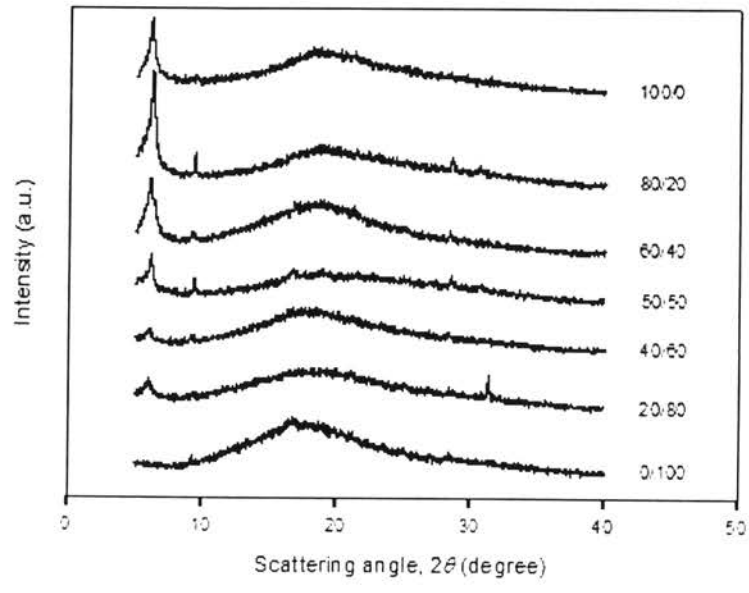
Intensity (a.u.)
100/0
80/20
60/40
50/50
40/60
20/80
0/100
0
10
20
30
40
50
Scattering angle, 2θ (degree)

(a)

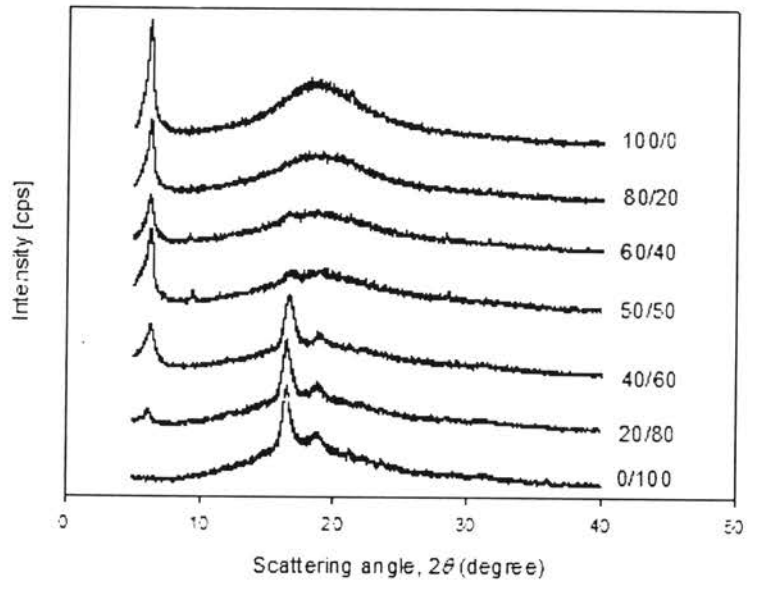
Intensity [cps]
100/0
80/20
60/40
50/50
40/60
20/80
0/100
0
10
20
30
40
50
Scattering angle, 2θ (degree)

(b)

Figure 7.7